Desalination and Water Treatment
www.deswater.com
doi: 10.5004/dwt.2020.25808

195 (2020) 305–313
August

Preparation of polyamine modified chitosan materials for reactive brilliant red removal from aqueous solutions

Jianlan Cui*, Xiao Wang, Siyuan Yu, Xin Wang, Congshan Zhong, Ning Wang, Jian Meng

School of Chemical Engineering and Technology, North University of China, Shanxi 030051, China, Tel. +8615513294306; emails: 414559203@qq.com (J. Cui), 2440582012@qq.com (X. Wang), yusiyuan_1995@163.com (S. Yu), 835995596@qq.com (X. Wang), 964288782@qq.com (C. Zhong), 2320997116@qq.com (N. Wang), mengjian379@139.com (J. Meng)

Received 21 July 2019; Accepted 7 March 2020

ABSTRACT

For effective dye removal from wastewater, chitosan was simultaneously cross-linked with polyethylenimine (PEI) and triethylenetetramine (TETA) to prepare two kinds of polyamine modified chitosan adsorbents PEI-CCTS and TETA-CCTS, respectively. The physicochemical properties of the obtained materials were characterized by Fourier-transform infrared spectroscopy, scanning electron microscopy, energy-dispersive X-ray spectroscopy, X-ray diffraction, and TGA. In adsorption experiments, TETA-CCTS and PEI-CCTS showed better adsorption performance for reactive brilliant red (RBR) compared with chemically cross-linked chitosan (CCTS), and the adsorption capacity per unit area was increased of 83.15% and 118.93%, respectively. The effects of experimental parameters such as pH and ionic strength on the absorption process of TETA-CCTS and PEI-CCTS for RBR were investigated in detail. The adsorption kinetics and equilibrium adsorption data of dye wastewater onto adsorbents were fitted with various models. All in all, TETA-CCTS and PEI-CCTS, with simple preparation methods and high adsorption capacity, were expected to be widely used for the treatment of dye wastewater.

Keywords: Chitosan; Adsorption; Polyethylenimine; Triethylenetetramine; Reactive brilliant red; Dye wastewater

1. Introduction

With the development of industrialization, the treatment of environmental pollutants has become a serious problem [1]. Synthetic dyes, with low production costs, bright colors, and high resistance towards environmental factors, have been widely used for most types of industrial applications [2]. However, these dyes, especially the azo ones and their degradation products are detrimental to the environment and human beings owing to their toxicity and carcinogenic effects [3]. Even with low concentrations of dyes, the water quality will be deteriorated exponentially, thereby affecting the aquatic ecosystem [4,5]. Therefore, it is urgent to search for an effective approach to remove the dyes from wastewater [6].

Recently, a series methods including coagulation/flocculation [7], biological oxidation [8], ion-exchange [9], photocatalytic degradation [10], and adsorption [11] have been employed into dye wastewater scavenging, among which, adsorption is considered as the most effective and economic one [12].

Among varieties of adsorbents, chitosan viewed as a suitable candidate has been extensively employed in various forms for dyes removal. As a natural polymer, chitosan has a series of advantages such as low cost, excellent biocompatibility, environmental friendliness, and antibacterial activity [13–15]. The presence of a large number of hydroxyl and amino functional groups in its polymer chain moiety exerts an outstanding ability to interact with a wide variety of molecules via physical and chemical forces [16].

* Corresponding author.

However, during adsorption, pure chitosan still has its own shortcomings including low mechanical strength, inadequate absorption sites, and finite adsorption surface, which seriously limits its application to be an effective adsorbent [17]. Therefore, it is necessary to remedy these intrinsic defects and further improve its adsorption capability.

In order to overcome these shortcomings, chemically cross-linked chitosan (CCTS) has been prepared by using some different cross-linking agents such as glutaraldehyde [18], epichlorohydrin [19], tripolyphosphate [20], ethylenediaminetetraacetic acid [21], adipic acid dihydrazide [22], and genipin [23]. Despite their merits, the adsorption capacity of CCTS will be decreased owing to the consumption of the amine and hydroxyl groups of chitosan during the cross-linking reaction [24]. For improving the efficiency of dyes extraction, to date, CCTS has been further modified with other materials such as poly(vinylbenzyl chloride – p-divinylbenzene), ethylenediaminetetraacetic acid, ethylenediamine, triethylenetetramine, xanthate and thiourea [16,25–28]. Among these modified methods, the introduction of active moieties onto chitosan, especially $-NH_2-$ or –NH–, causes a great affinity for removing anionic dyes from aqueous solutions. In this study, aminated chitosan materials were prepared by simultaneous cross-linking of polyamine reagents polyethylenimine (PEI) and triethylenetetramine (TETA) respectively, and utilized into reactive brilliant red (RBR) removal from aqueous solutions. The chemical processes for preparing the adsorbents are presented in Fig. 1.

2. Experimental setup

2.1. Reagents and instruments

Chitosan (CTS, deacetylation degree ≥ 90%, <200 mPa s), hydrochloric acid (HCl, 36%–38%), sodium hydroxide (NaOH), sodium chloride (NaCl) and acetic acid (AA) were purchased from Sinopharm Chemical Reagent Co. Ltd., (China); glutaraldehyde (GA, 50% in water) was purchased from Beijing Huawei Ruike Chemical Co., Ltd., (Beijing, China); polyethylenimine (PEI, molecular weight of 2×10^4–5×10^4) was purchased from Wuhan Qionglong Chemical New Material Co., Ltd., (Wuhan, China); TETA was purchased from Shanghai Meryer Chemical Technology Co., Ltd. (Shanghai, China); RBR was purchased from Shanghai Jiaying Chemical Co., Ltd. (Shanghai, China); deionized water was prepared in the laboratory.

Fourier-transform infrared spectrometer (FTIR, Spectrum Two, USA); scanning electron microscope (SEM, SU8010, Japan); laser particle size distribution analyzer (BT-2002, Dandong Bettersize, China); X-ray diffraction (XRD, Dandong Haoyuan, China); UV-visible spectrophotometer (UV-2602, China) were used as analytical instruments.

2.2. Preparation of TETA-CCTS

CTS powder (2 g) was sufficiently mixed with an acetic acid solution (100 mL, 2%) by stirring. TETA (0.25 mL) was dissolved in deionized water (5 mL), then adjusted the

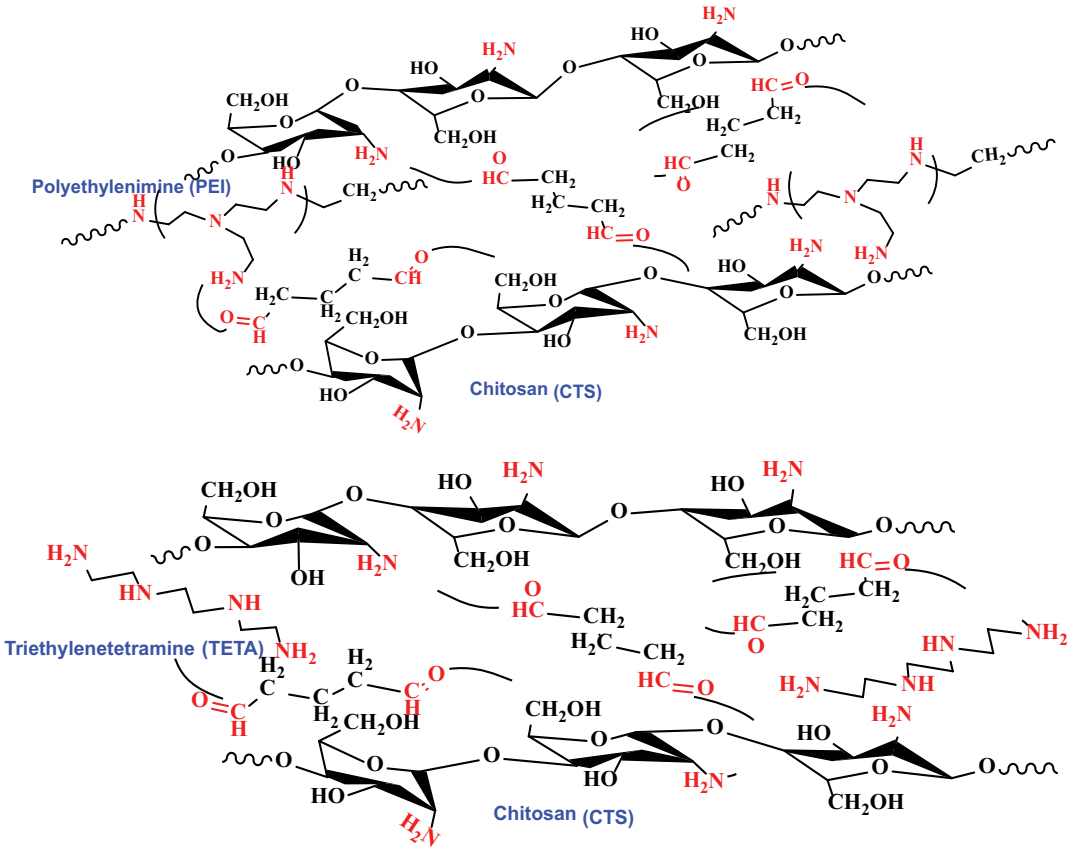

Fig. 1. Chemical process for preparing functional polyaminated adsorbents PEI-CCTS and TETA-CCTS.

pH of the solution to weakly acidic with 1 mL acetic acid, followed by adding the prepared CTS-acetic acid solution and treated with ultrasound. Subsequently, a GA solution (2 mL, 25%) was added and continued to stir at 40°C for 2 h, then added 1 mol L^{-1} NaOH solution and further reacted for 2 h. The obtained solid product was washed with water and ethanol repeatedly and dried at 45°C under vacuum, thus, successfully preparing TETA-CCTS.

2.3. Preparation of PEI-CCTS

The preparation process of PEI-CCTS was similar to that of TETA-CCTS. In brief, PEI (1 mL) was dissolved in deionized water (5 mL), and the pH of the solution was adjusted to weak acid using acetic acid (1 mL), then added with the prepared CTS-acetic acid solution and treated under ultrasound for 30 min. A GA solution (2 mL, 25%) was added to the mixture and stirred for 2 h, followed by adding a NaOH solution (1 mol L^{-1}) and reacted for another 2 h to obtain the precipitate. After filtration, washed with water and ethanol, as well as dried, PEI-CCTS was successfully prepared.

2.4. Adsorption experiments

A stock solution of 2,000 mg L^{-1} RBR was prepared and diluted with deionized water into diverse concentrations. The adsorption kinetics and adsorption thermodynamics of CCTS, TETA-CCTS, and PEI-CCTS were systematically investigated.

A total of 4 mg prepared adsorbents were added to a number of 50 mL conical flasks, then the RBR solution (40 mL) was added into these flasks. The flasks were placed in a thermostat shaker of 20°C and shaken at 120 rpm. A conical flask was taken at intervals and the corresponding concentration was determined by UV. The adsorption capacities of the adsorbents were calculated by Eq. (1), thereby investigating the adsorption kinetics.

$$Q_t = \frac{V\left(C_0 - C_t\right)}{m} \tag{1}$$

where Q_t (mg g^{-1}) is the adsorption amount at t moment; V (mL) is the volume of the adsorbate; m (g) is the mass of the adsorbent; C_0 and C_t (mg L^{-1}) are the concentration of dye solution at the initial time and t moment, respectively.

The prepared adsorbents (4 mg) were added into a 40 mL dye solution with different concentrations. The isothermal adsorption experiments were performed in a constant temperature oscillator at 120 rpm. After adsorption saturation, the concentration of the dye solution in the supernatant was determined by UV. The equilibrium adsorption amount was calculated according to Eq. (2).

$$Q_e = \frac{V\left(C_0 - C_e\right)}{m} \tag{2}$$

where Q_e (mg g^{-1}) is the equilibrium adsorption amount; V (mL) is the volume of the adsorbate; m (g) is the mass of the adsorbent; C_0 and C_e (mg L^{-1}) are the initial and equilibrium concentration of dye solution, respectively.

3. Result and discussion

3.1. Characterization of adsorbents

Fig. 2 shows the infrared spectra of CCTS, TETA-CCTS, and PEI-CCTS. In the spectrum of CCTS (Fig. 2c), the broad peak near 3,430 cm^{-1} was the stretching vibration of −OH and $-NH_2$, which also confirmed the presence of the hydrogen bond in the molecular structure. The bending vibration of the amine group in the chitosan molecular generated an absorption peak at a wavelength of 1,603 cm^{-1}. For those polyamine modified adsorbents, PEI-CCTS (Fig. 2a), and TETA-CCTS (Fig. 2b), the peak at 1,597 cm^{-1} shifted to 1,573 and 1,574 cm^{-1} respectively, indicating that the amino group was involved in the reaction [29].

Fig. 3 shows the scanning electron microscopy images of CCTS, TETA-CCTS, and PEI-CCTS. As shown in Fig. 3, all three adsorbents are irregular in shape and have relatively tight surfaces.

The N content of the three kinds of adsorbents was analyzed by energy-dispersive X-ray spectroscopy (Fig. 4). After the cross-linking reaction, the N content of PEI-CCTS and TETA-CCTS was increased between 9.9% and 6.5%, respectively compared with that of CCTS.

As shown in Fig. 5, the particle size distribution of TETA-CCTS and PEI-CCTS is relatively narrow, mainly concentrating at 151 and 184 μm, respectively. In contrast, CCTS has a wide particle size distribution. In addition, the surface areas of CCTS, TETA-CCTS, and PEI-CCTS are 0.10, 0.05, and 0.04 $m^2\ g^{-1}$, respectively.

As presented in Fig. 6, all three adsorbents have an obvious diffraction peak at 20.14°, which can be attributed to the regular arrangement of the chitosan chain segment [30]. Compared with CTS powder, the diffraction peak intensity of CCTS at 20.14° became weak, which may be due to the fact that the regularity of the chitosan chain was

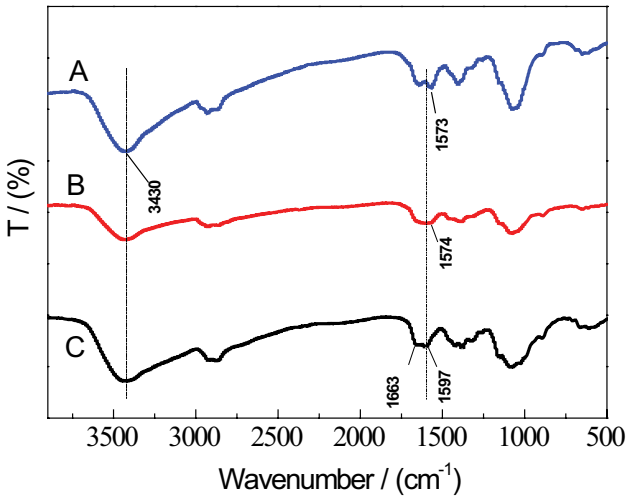

Fig. 2. Fourier-transform infrared spectroscopy spectra of three adsorbents (a) PEI-CCTS, (b) TETA-CCTS, and (c) CCTS.

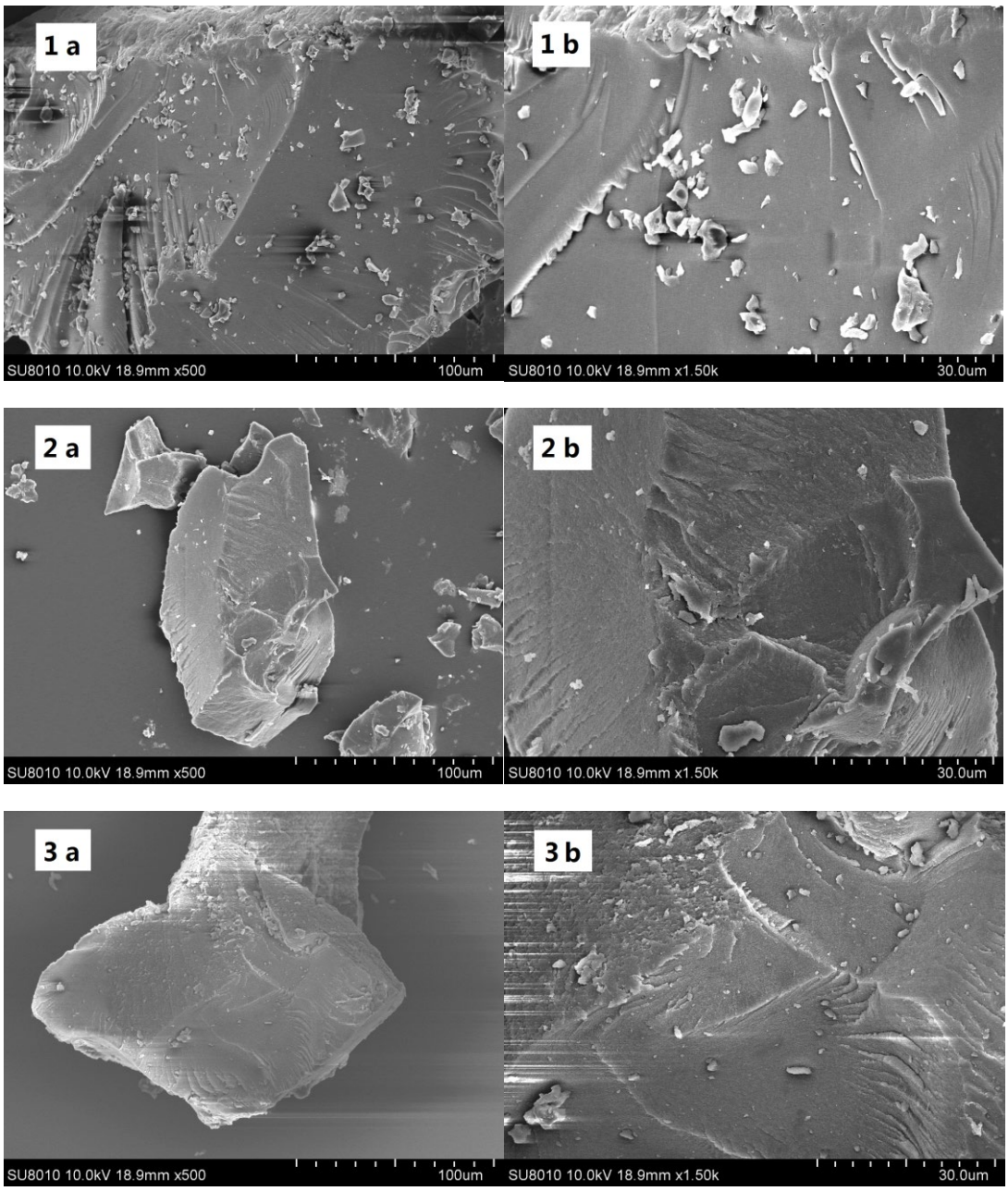

Fig. 3. Scanning electronic microscopy images of (1a and 1b) CCTS, (2a and 2b) TETA-CCTS, and (3a and 3b) PEI-CCTS.

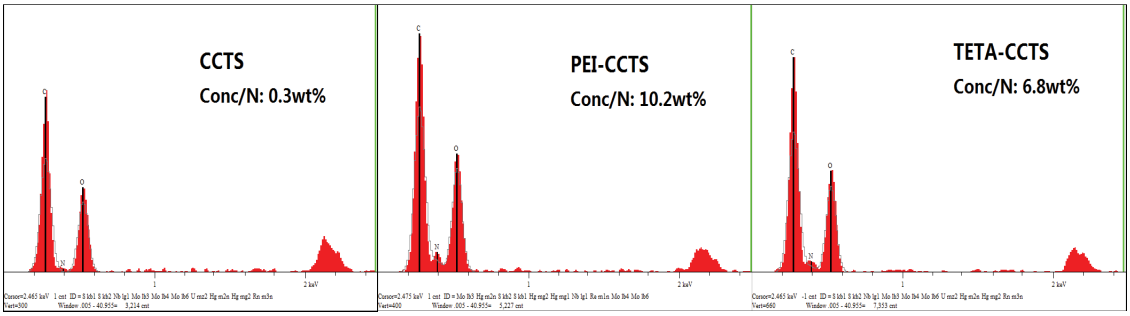

Fig. 4. Energy-dispersive X-ray spectroscopy of CCTS, PEI-CCTS, and TETA-CCTS.

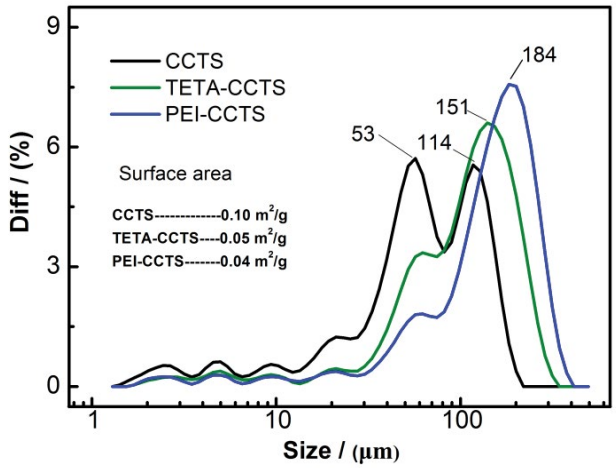

Fig. 5. Particle size distribution of CCTS, TETA-CCTS, and PEI-CCTS.

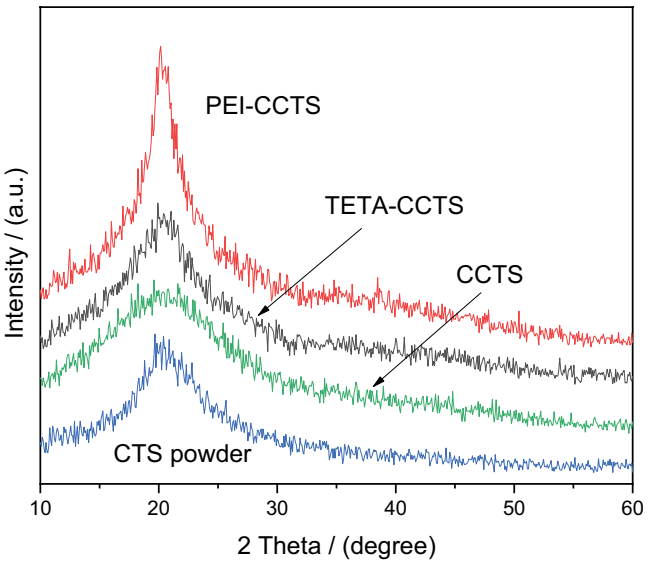

Fig. 6. X-ray diffraction patterns of CTS powder, CCTS, TETA-CCTS, and PEI-CCTS.

reduced by the cross-linking reaction, thereby resulting in a decrease in the crystallinity [31]. In addition, the diffraction peak intensity of TETA-CCTS and PEI-CCTS at 20.14° enhanced. This may be because a large number of hydrogen bonds can be formed during the process of simultaneous cross-linking with aminated substance, thereby leading to an increase in the crystallinity. Furthermore, as a macromolecular compound, PEI possesses the specific properties of the polymer. Therefore, the diffraction peak intensity of PEI-CCTS was stronger than that of TETA-CCTS.

From Fig. 7, the TGA curves of CTS powder, CCTS, TETA-CCTS, and PEI-CCTS can be divided into three weight-loss stages. The first weight-loss stage, below 200°C, was due to the evaporation of the adsorbed water [32]. The temperature from 200°C to 400°C was the second stage of weight-loss, which can be attributed to the decomposition of the acetyl in

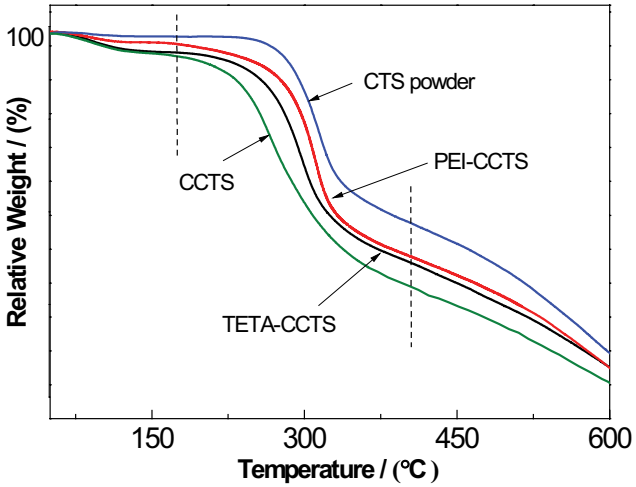

Fig. 7. TGA patterns of CTS powder, CCTS, TETA-CCTS, and PEI-CCTS.

the main chain of chitosan molecules. The third weight-loss stage, higher than 400°C, was possibly caused by the decomposition of the chitosan main chain. Compared with CTS powder, the regularity of the chitosan chain for CCTS, TETA-CCTS, and PEI-CCTS was destroyed by the cross-linking reaction, thereby decreasing their degradation temperature.

3.2. Study on adsorption properties of microspheres

3.2.1. Study on adsorption kinetics

Fig. 8 depicts the adsorption kinetics curves of CCTS, TETA-CCTS, and PEI-CCTS for anionic dye RBR. It can be seen that the adsorption amount of CCTS, TETA-CCTS, and PEI-CCTS for RBR in 3 h reached 320.55, 180.15, and 250.17 mg g^{-1}, respectively.

To further explore the adsorption kinetics process of three particles on dye wastewater, pseudo-first-order kinetic model and pseudo-second-order kinetic model was utilized to fit the adsorption kinetics data according to Eqs. (3) and (4) [33].

Pseudo-first-order kinetic equation:

$$\ln(Q_e - Q_t) = \ln Q_e - k_1 t \tag{3}$$

Pseudo-second-order kinetic equation:

$$\frac{t}{Q_t} = \frac{1}{k_2 Q_e^2} + \frac{t}{Q_e} \tag{4}$$

where Q_t and Q_e are the adsorption capacities at t moment and adsorption equilibrium, respectively; k_1 and k_2 are equilibrium adsorption rate constant.

As shown in Table 1, a high linear correlation coefficient R^2 can be obtained by fitting with both pseudo-first-order and pseudo-second-order kinetic models for PEI-CCTS, and the equilibrium adsorption capacity Q_e obtained by the pseudo-second-order kinetic model is closer to the experimental value $Q_{experimental}$. For TETA-CCTS, the linear

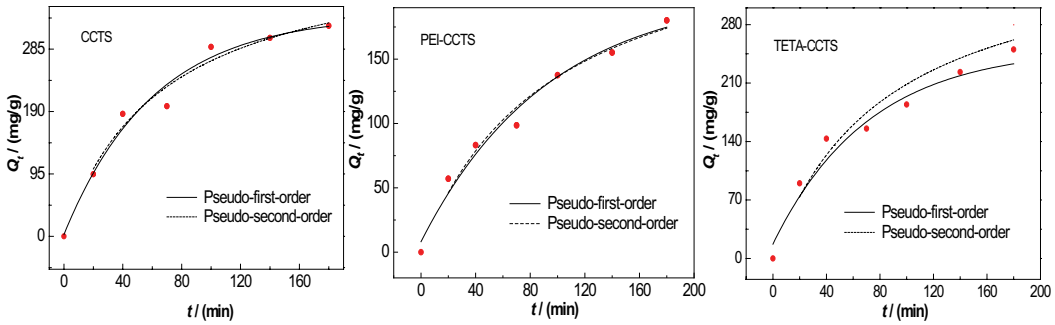

Fig. 8. Effect of adsorption time on adsorption capacity of CCTS, TETA-CCTS, and PEI-CCTS for RBR; pseudo-first/second-order kinetic model.

Table 1
Adsorption kinetic parameters of CCTS, TETA-CCTS, and PEI-CCTS

	$Q_{experimental}$ (mg g^{-1})	Pseudo-first-order kinetic model			Pseudo-second-order kinetic model		
		Q_e (mg g^{-1})	k_1 min^{-1}	R^2	Q_e (mg g^{-1})	k_2 (g mg^{-1} min^{-1})	R^2
CCTS	347.77	334.32	0.0164	0.966	445.63	3.36×10^{-5}	0.940
PEI-CCTS	304.55	203.20	0.0107	0.971	266.31	3.94×10^{-5}	0.956
TETA-CCTS	318.47	252.15	0.0140	0.786	383.63	3.11×10^{-5}	0.869

coefficient derived from the pseudo-second-order model is higher than that fitted with the pseudo-first-order model. The results indicated that the adsorption process of RBR by PEI-CCTS and TETA-CCTS was mainly controlled by chemical adsorption. According to the surface areas of three particles (Fig. 5), it was calculated that the adsorption capacities of CCTS, TETA-CCTS, and PEI-CCTS for RBR were 3,477.7; 6,369.4; and 7,613.75 mg m^{-2}, respectively. Therefore, it can be concluded that PEI-CCTS showed the best adsorption performance.

3.2.2. Effect of pH value and ionic strength

Fig. 9 represents the adsorption capacities of CCTS, PEI-CCTS, and TETA-CCTS for RBR under different pH. The maximum adsorption amount of PEI-CCTS and TETA-CCTS reached 323.30 and 340.01 mg g^{-1} when pH was 2. With the increase of pH, the adsorption capacities decreased. The amino groups on the adsorbents were in protonation state under acidic condition, thereby easily combining with negatively charged RBR via coulomb force. Due to the cross-linking of TETA and PEI with CTS, the number of amino groups increased, resulting in a higher degree of protonation of TETA-CCTS and PEI-CCTS in the acidic environment compared with CCTS. However, in an alkaline environment, the degree of protonation of amino groups on the surface of the adsorbent decreased, which resulted in a decrease in the adsorption capacities of RBR.

The adsorption abilities of the adsorbents for RBR were investigated at various ionic strength and the results are presented in Fig. 10. The adsorption capacities of three adsorbents decreased with the increase of NaCl concentration in solution. When the concentration of NaCl in the solution increased from 0 to 0.1 mol L^{-1}, the adsorption capacities of PEI-CCTS and TETA-CCTS for RBR decreased by 10.21% and 5.30%, respectively. The reason may be that a large amount of Cl^- and Na^+ in the solution will compete with the dye for adsorption, and weaken the adsorption effect of the adsorbents, eventually leading to a decrease in the amount of the adsorption [34].

3.2.3. Isothermal adsorption study and parameter fitting

As shown in Fig. 11, the adsorption capacity of TETA-CCTS for RBR increases with the increase of the initial concentration of dye. In addition, the temperature increase also generates an active effect on the adsorption amount of RBR by TETA-CCTS, which indicates that adsorption is an endothermic process. The isothermal adsorption data were fitted with different isothermal adsorption data, and the corresponding formulas are as follows [35–37]:

Langmuir isothermal equation:

$$\frac{C_e}{Q_e} = \frac{1}{b_L Q_m} + \frac{C_e}{Q_m} \tag{5}$$

$$b_L = (K-1) \times \frac{M}{\rho} \tag{6}$$

$$R_L = \frac{1}{\left(bC_0 + 1\right)} \tag{7}$$

Freundlich isothermal equation:

$$\ln Q_e = \ln K_F + \frac{\ln C_e}{n} \tag{8}$$

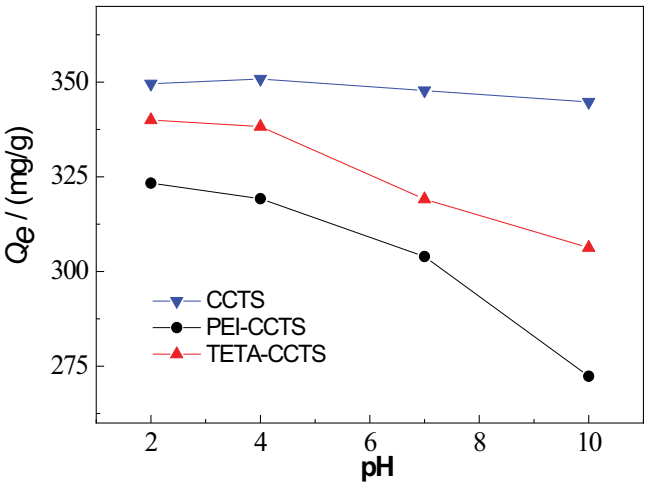

Fig. 9. Effect of pH on adsorption capacities.

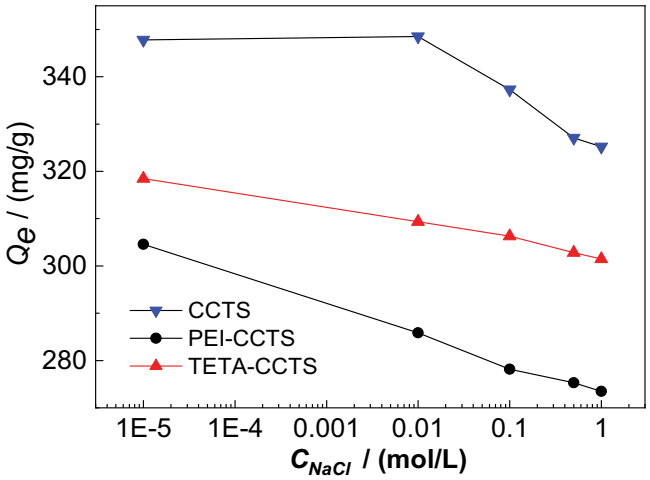

Fig. 10. Effect of ionic strength on adsorption capacities.

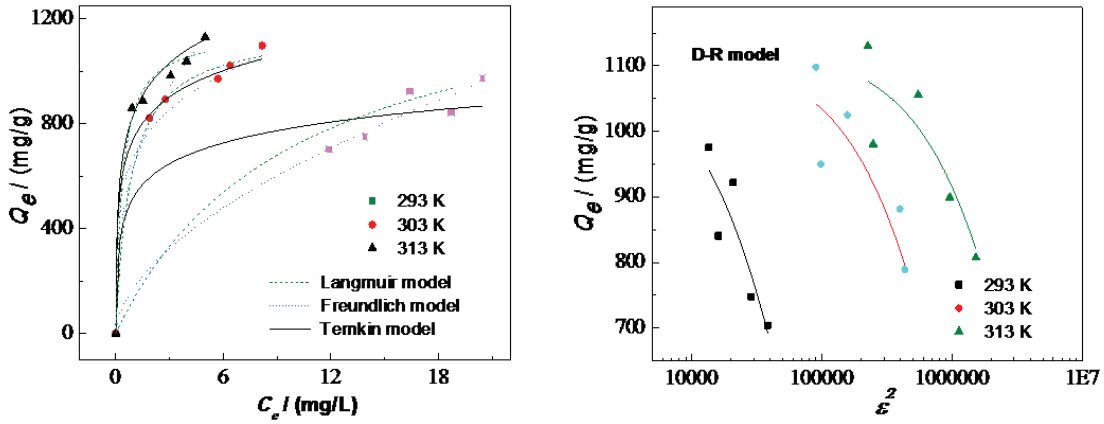

Fig. 11. Adsorption isotherms of RBR adsorption by TETA-CCTS at different temperatures; Langmuir, Freundlich, Dubinin–Radushkevitch isotherm, and Temkin model of RBR adsorption on TETA-CCTS.

Dubinin–Radushkevitch isothermal equation:

$$\ln Q_e = \ln Q_m - K_D \varepsilon^2 \tag{9}$$

$$\varepsilon = RT \ln\left(1 + \frac{1}{C_e}\right) \tag{10}$$

$$E = \frac{1}{\sqrt{-2K_D}} \tag{11}$$

Temkin isotherm equation:

$$Q_e = \frac{RT}{b_T} \ln\left(K_T C_e\right) \tag{12}$$

The fitting parameters obtained from the four isothermal adsorption models are listed in Table 2. Langmuir isothermal adsorption model showed the best fitting performance, the R^2 value at 20°C, 30°C, and 40°C reached 0.995, 0.994, and 0.986, respectively. The values of R_L at different temperatures were all between 0 and 1, indicating that the conditions were favorable for adsorption [38]. In addition, the $1/n$ values of the Freundlich fitting parameters were all between 0 and 1 at different temperatures, illustrating that the adsorption process was preferential adsorption. Furthermore, Gibbs free energy ΔG was calculated according to the equilibrium constant K at different temperatures, and the values of ΔH and ΔS were calculated by Van't Hoff equation [39].

$$\Delta G = -RT \ln K \tag{13}$$

$$\ln K = -\frac{\Delta H}{RT} + \frac{\Delta S}{R} \tag{14}$$

Table 3 shows the thermodynamic data of the adsorption process. The negative values of ΔG at different temperatures indicated that the adsorption process was spontaneous.

Table 2
Parameters of isotherm models of RBR adsorption by TETA-CCTS

Model	Parameter	T (°C)		
		20	30	40
Langmuir	Q_m (mg g^{-1})	1,428.04	1,163.05	1,151.38
	b_L (L mg^{-1})	0.060	1.205	2.695
	R_L	0.109–0.168	0.006–0.010	0.003–0.004
	K	1.0033	1.0669	1.1497
	R^2	0.995	0.994	0.986
Freundlich	K_F (L mg^{-1})	174.58	672.59	631.19
	$1/n$	0.5635	0.2161	0.3596
	R^2	0.977	0.735	0.928
Dubinin–Radushkevitch	Q_m (mg g^{-1})	1,110.8	1,118.2	1,127.9
	K_D	1.2283	7.837	2.089
	R^2	0.711	0.659	0.638
Temkin	b_T (J mol^{-1})	21.18	17.45	14.67
	K_T	92.61	172.32	111.2
	R^2	0.933	0.862	0.974

Table 3
Thermodynamics parameters at different temperatures

T (°C)	ΔG (kJ mol^{-1})	ΔH (kJ mol^{-1})	ΔS (J K^{-1} mol^{-1})
20	–8.03		
30	–163.13	5.18×10^{-3}	17.70
40	–363.02		

The absolute values of ΔG increased with the increase of the temperature, indicating that the temperature rise was beneficial for adsorption. The positive values of ΔH and ΔS illustrated that the adsorption was an endothermic process, and the degree of freedom in the solid-liquid interface increased during the adsorption.

4. Conclusions

In order to effectively remove RBR from aqueous solutions, PEI and TETA were simultaneously cross-linked with chitosan to prepare aminated adsorbents PEI-CCTS and TETA-CCTS, respectively. Characterization of two adsorbents using various techniques confirmed their successful preparation. The adsorption experiments indicated that both PEI-CCTS and TETA-CCTS were effective adsorbents for the treatment of RBR in aqueous solutions. The increase of pH, as well as, ionic strength, will cause an adverse effect on the adsorption capacity of aminated particles for RBR removal. Furthermore, the adsorption kinetics and isotherms of RBR on PEI-CCTS and TETA-CCTS followed the pseudo-second-order kinetic model and Langmuir isotherm model, respectively. The negative value of ΔG confirmed that the adsorption process was spontaneous. Based on the experiment results, it was concluded that the adsorption processes of RBR by PEI-CCTS and TETA-CCTS were mainly controlled by chemical adsorption.

References

[1] R. Castaldo, R. Avolio, M. Cocca, G. Gentile, M.E. Errico, M. Avella, C. Carfagna, V. Ambrogi, A versatile synthetic approach toward hyper-cross-linked styrene-based polymers and nanocomposites, Macromolecules, 50 (2017) 4132–4143.
[2] W.S.W. Ngah, L.C. Teong, M.A.K.M. Hanafiah, Adsorption of dyes and heavy metal ions by chitosan composites: a review, Carbohydr. Polym., 83 (2011) 1446–1456.
[3] P. Semeraro, V. Rizzi, P. Fini, S. Matera, P. Cosma, E. Franco, R. García, M. Ferrándiz, E. Núñez, J.A. Gabaldón, I. Fortea, E. Pérez, M. Ferrándiz, Interaction between industrial textile dyes and cyclodextrins, Dyes Pigm., 119 (2015) 84–94.
[4] J.P. Zhao, W.C. Ren, H.-M. Cheng, Graphene sponge for efficient and repeatable adsorption and desorption of water contaminations, J. Mater. Chem., 22 (2012) 20197–20202.
[5] J.E. Aguiar, J.C.A. de Oliveira, P.F.G. Silvino, J.A. Neto, I.J. Silva Jr., S.M.P. Lucena, Correlation between PSD and adsorption of anionic dyes with different molecular weigths on activated carbon, Colloids Surf., A, 496 (2016) 125–131.
[6] M.T. Yagub, T.K. Sen, S. Afroze, H.M. Ang, Dye and its removal from aqueous solution by adsorption: a review, Adv. Colloid Interface Sci., 209 (2014) 172–184.
[7] C.C. Mólgora, A.M. Domínguez, E.M. Avila, P. Drogui, G. Buelna, Removal of arsenic from drinking water: a comparative study between electrocoagulation-microfiltration and chemical coagulation-microfiltration processes, Sep. Purif. Technol., 118 (2013) 645–651.
[8] H.F. Zhuang, H.J. Han, S.Y. Jia, B.L. Hou, Q. Zhao, Advanced treatment of biologically pretreated coal gasification wastewater by a novel integration of heterogeneous catalytic ozonation and biological process, Bioresour. Technol., 166 (2014) 592–595.
[9] S.J. Lim, T.H. Kim, Combined treatment of swine wastewater by electron beam irradiation and ion-exchange biological reactor system, Sep. Purif. Technol., 146 (2015) 42–49.
[10] T.T. Zhu, Y.H. Song, H.Y. Ji, Y.G. Xu, Y.X. Song, J.X. Xia, S. Yin, Y.P. Li, H. Xu, Q. Zhang, H.M. Li, Synthesis of g-C_3N_4/Ag_3VO_4 composites with enhanced photocatalytic activity under visible light irradiation, Chem. Eng. J., 271 (2015) 96–105.
[11] Y.Y. Sun, J.B. Zhou, W.Q. Cai, R.S. Zhao, J.P. Yuan, Hierarchically porous NiAl-LDH nanoparticles as highly efficient adsorbent for p-nitrophenol from water, Appl. Surf. Sci., 349 (2015) 897–903.
[12] B. Yu, B. Yang, G.L. Li, H.L. Cong, Preparation of monodisperse cross-linked poly(glycidyl methacrylate)@Fe_3O_4@diazoresin

magnetic microspheres with dye removal property, J. Mater. Sci., 53 (2018) 6471–6481.
[13] İ. Sargın, M. Kaya, G. Arslan, T. Baran, T. Ceter, Preparation and characterisation of biodegradable pollen–chitosan microcapsules and its application in heavy metal removal, Bioresour. Technol., 177 (2015) 1–7.
[14] S.J. Jeon, Z.X. Ma, M.Y. Kang, K.N. Galvão, K.C. Jeong, Application of chitosan microparticles for treatment of metritis and in vivo evaluation of broad spectrum antimicrobial activity in cow uteri, Biomaterials, 110 (2016) 71–80.
[15] V. Zargar, M. Asghari, A. Dashti, A review on chitin and chitosan polymers: structure, chemistry, solubility, derivatives, and applications, ChemBioEng Rev., 2 (2015) 204–226.
[16] X.-j. Hu, J.-s. Wang, Y.-g. Liu, X. Li, G.-m. Zeng, Z.-l. Bao, X.-x. Zeng, A.-w. Chen, F. Long, Adsorption of chromium(VI) by ethylenediamine-modified cross-linked magnetic chitosan resin: isotherms, kinetics and thermodynamics, J. Hazard. Mater., 185 (2011) 306–314.
[17] C.K.S. Pillai, W. Paul, C.P. Sharma, Chitin and chitosan polymers: chemistry, solubility and fiber formation, Prog. Polym. Sci., 34 (2009) 641–678.
[18] C.Z. Fan, K. Li, J.X. Li, D.W. Ying, Y.L. Wang, J.P. Jia, Comparative and competitive adsorption of Pb(II) and Cu(II) using tetraethylenepentamine modified chitosan/$CoFe_2O_4$ particles, J. Hazard. Mater., 326 (2017) 211–220.
[19] G.Z. Kyzas, P.I. Siafaka, D.A. Lambropoulou, N.K. Lazaridis, D.N. Bikiaris, Poly (itaconic acid)-grafted chitosan adsorbents with different cross-linking for Pb(II) and Cd(II) uptake, Langmuir, 30 (2014) 120–131.
[20] E.S. Dragan, D.F. Apopei Loghin, A.I. Cocarta, Efficient sorption of Cu^{2+} by composite chelating sorbents based on potato starch-graft-polyamidoxime embedded in chitosan beads, ACS Appl. Mater. Interfaces, 6 (2014) 16577–16592.
[21] F.P. Zhao, E. Repo, M. Sillanpää, Y. Meng, D.L. Yin, W.Z. Tang, Green synthesis of magnetic EDTA- and/or DTPA-cross-linked chitosan adsorbents for highly efficient removal of metals, Ind. Eng. Chem. Res., 54 (2015) 1271–1281.
[22] E.D. Zheng, Q.F. Dang, C.S. Liu, B. Fan, J.Q. Yan, Z.Z. Yu, H.F. Zhang, Preparation and evaluation of adipic acid dihydrazide cross-linked carboxymethyl chitosan microspheres for copper ion adsorption, Colloids Surf., A, 502 (2016) 34–43.
[23] L.S. Rocha, Â. Almeida, C. Nunes, B. Henriques, M.A. Coimbra, C.B. Lopes, C.M. Silva, A.C. Duarte, E. Pereira, Simple and effective chitosan based films for the removal of Hg from waters: equilibrium, kinetic and ionic competition, Chem. Eng. J., 300 (2016) 217–229.
[24] S.-P. Kuang, Z.-Z. Wang, J. Liu, Z.-C. Wu, Preparation of triethylene-tetramine grafted magnetic chitosan for adsorption of Pb(II) ion from aqueous solutions, J. Hazard. Mater., 260 (2013) 210–219.
[25] M.S. de Luna, R. Castaldo, R. Altobelli, L. Gioiella, G. Filippone, G. Gentile, V. Ambrogi, Chitosan hydrogels embedding hypercrosslinked polymer particles as reusable broad-spectrum adsorbents for dye removal, Carbohydr. Polym., 177 (2017) 347–354.
[26] S. Fujita, N. Sakairi, Water soluble EDTA-linked chitosan as a zwitterionic flocculant for pH sensitive removal of Cu(II) ion, RSC Adv., 6 (2016) 10385–10392.
[27] N. Wang, X.J. Xu, H.Y. Li, L.Z. Yuan, H.W. Yu, Enhanced selective adsorption of Pb(II) from aqueous solutions by one-pot synthesis of xanthate-modified chitosan sponge: behaviors and mechanisms, Ind. Eng. Chem. Res., 55 (2016) 12222–12231.
[28] L.M. Zhou, J.H. Liu, Z.R. Liu, Adsorption of platinum(IV) and palladium(II) from aqueous solution by thiourea-modified chitosan microspheres, J. Hazard. Mater., 172 (2009) 439–446.
[29] Z.-X. Xue, G.-P. Yang, Z.-P. Zhang, B.-L. He, Application of chitosan microspheres as carriers of LH-RH analogue TX46, React. Funct. Polym., 66 (2006) 893–901.
[30] H.F. Zhang, Q.F. Dang, C.S. Liu, D.J. Yu, Y. Wang, X.Y. Pu, Y. Liu, Y.Y. Liang, D.S. Cha, Fabrication of methyl acrylate and tetraethylenepentamine grafted magnetic chitosan microparticles for capture of Cd(II) from aqueous solutions, J. Hazard. Mater., 366 (2019) 346–357.
[31] M.J. Xie, L.X. Zeng, Q.Y. Zhang, Y. Kang, H.J. Xiao, Y. Peng, X.C. Chen, J.W. Luo, Zhang Q.Y., Synthesis and adsorption behavior of magnetic microspheres based on chitosan/organic rectorite for low-concentration heavy metal removal, J. Alloys Compd., 647 (2015) 892–905.
[32] W. Ma, J.D. Dai, X.H. Dai, Z.L. Da, Y.S. Yan, Core–shell molecularly imprinted polymers based on magnetic chitosan microspheres for chloramphenicol selective adsorption, Monatsh. Chem., 3 (2015) 465–474.
33] H.F. Zhang, Q.F. Dang, C.S. Liu, D.S. Cha, Z.Z. Yu, W.J. Zhu, B. Fan, Uptake of Pb(II) and Cd(II) on chitosan microsphere surface successively grafted by methyl acrylate and diethylenetriamine, ACS Appl. Mater. Interfaces, 9 (2017) 11144–11155.
[34] A.Z.M. Badruddoza, Z.B.Z. Shawon, W.J.D. Tay, K. Hidajat, M.S. Uddin, Fe_3O_4/cyclodextrin polymer nanocomposites for selective heavy metals removal from industrial wastewater, Carbohydr. Polym., 91 (2013) 322–332.
[35] T. Trakulsujaritchok, N. Noiphom, N. Tangtreamjitmun, R. Saeeng, Adsorptive features of poly(glycidyl methacrylate-co-hydroxyethyl methacrylate): effect of porogen formulation on heavy metal ion adsorption, J. Mater. Sci., 46 (2011) 5350–5362.
[36] X.L. Li, Y.X. Qi, Y.F. Li, Y. Zhang, X.H. He, Y.H. Wang, Novel magnetic beads based on sodium alginate gel crosslinked by zirconium(IV) and their effective removal for Pb^{2+} in aqueous solutions by using a batch and continuous systems, Bioresour. Technol., 142 (2013) 611–619.
[37] L. Bai, H.P. Hu, W. Fu, J. Wan, X.L. Cheng, L. Zhuge, L. Xiong, Q.Y. Chen, Synthesis of a novel silica-supported dithiocarbamate adsorbent and its properties for the removal of heavy metal ions, J. Hazard. Mater., 195 (2011) 261–275.
[38] J. Meng, J.L. Cui, J. Yu, W. Huang, P. Wang, K. Wang, M.Q. Liu, C.Y. Song, P. Chen, Preparation of green chelating fibers and adsorption properties for Cd(II) in aqueous solution, J. Mater. Sci., 53 (2018) 2277–2289.
[39] S.Y. Yu, J.L. Cui, H. Jiang, C.S. Zhong, J. Meng, Facile fabrication of functional chitosan microspheres and study on their effective cationic/anionic dyes removal from aqueous solution, Int. J. Biol. Macromol., 99 (2019) 7573–7586.